Check for updates

†These authors have contributed equally to this work and share first authorship

‡These authors have contributed equally to this work and share last authorship

Oxygen level is a critical regulator of human B cell differentiation and IgG class switch recombination

Jana Koers[1†], Casper Marsman[1†], Juulke Steuten[1†], Simon Tol[2], Ninotska I. L. Derksen[1], Anja ten Brinke[1], S. Marieke van Ham[1,3‡] and Theo Rispens[1*‡]

[1]Department of Immunopathology, and Landsteiner Laboratory, Sanquin Research, Amsterdam University Medical Centers, University of Amsterdam, Amsterdam, Netherlands, [2]Department of Research Facilities, and Landsteiner Laboratory, Sanquin Research, Amsterdam University Medical Centers, University of Amsterdam, Amsterdam, Netherlands, [3]Swammerdam Institute for Life Sciences, University of Amsterdam, Amsterdam, Netherlands

The generation of high-affinity antibodies requires an efficient germinal center (GC) response. As differentiating B cells cycle between GC dark and light zones they encounter different oxygen pressures (pO_2). However, it is essentially unknown if and how variations in pO_2 affect B cell differentiation, in particular for humans. Using optimized *in vitro* cultures together with in-depth assessment of B cell phenotype and signaling pathways, we show that oxygen is a critical regulator of human naive B cell differentiation and class switch recombination. Normoxia promotes differentiation into functional antibody secreting cells, while a population of CD27^{++} B cells was uniquely generated under hypoxia. Moreover, time-dependent transitions between hypoxic and normoxic pO_2 during culture - reminiscent of *in vivo* GC cyclic re-entry - steer different human B cell differentiation trajectories and IgG class switch recombination. Taken together, we identified multiple mechanisms trough which oxygen pressure governs human B cell differentiation.

KEYWORDS

B cells, hypoxia, germinal center, differentiation, antibody-secreting cell, class switch recombination

Introduction

Development of an effective long-lasting immune response implies development of high-affinity, class-switched antibodies, the result of B cell differentiation within so-called germinal centers (GC), specialized substructures in secondary lymphoid tissues. Upon initiation of the humoral immune responses, initial T cell-dependent B cell activation

leads to generation of a GC response, which is preceded by a short period of extrafollicular B cell activation. During the initial extrafollicular response, an early wave of naive B cells differentiate into plasma blasts and early memory B cells. These cells display limited levels of somatic hypermutation and affinity maturation (1–4). The GC forms approximately one week after antigen exposure and becomes organized into two histologically distinct regions; the dark zone, where B cells undergo extensive proliferation and somatic hypermutation, and the light zone, where high-affinity B cells compete for antigen in order to undergo affinity selection. Class switch recombination may occur as early as the pre-GC stages and ensues in the GC reactions (5–7). GC B cells cycle repeatedly through the light zone and dark zone. After initial fate decision, differentiation may proceed towards affinity-matured late memory B cells or antibody secreting cells (i.e., plasmablasts and plasma cells) with accumulating affinity maturation (8–10).

Previous studies by ourselves and others using *in vitro* cultures of human or mouse B cells demonstrated that a GC-like B cell response can be faithfully reproduced, including generation of mature memory B cells and antibody secreting cells (11, 12). Similar to what has been reported *in vivo*, CD40 ligation together with the availability of Tfh-associated cytokines IL-4 and IL-21 is required to promote B cell proliferation, isotype switching and generation of antibody secreting cell *in vitro* (2, 13–15). The combined action of Tfh-derived CD40L, IL-21, and IL-4, results in activation of NFκB and JAK-STAT pathways. These are vital for, amongst others, upregulation of BLIMP1 and XBP-1s, transcription factors necessary for initiation of antibody secreting cell differentiation and antibody production (16–20), as well as C-Myc and IRF4 upregulation (18, 21–23). C-Myc is required for the survival of GC B cells and is strongly upregulated upon antigen-specific selection in the GC light zone, allowing for dark zone (re-) entry (24–27). A central role in orchestrating these events is the transcriptional repressor BCL6, which regulates expression of amongst others c-Myc and BLIMP1 (24, 28, 29) (For more detail, see Figure S4A).

The partial pressure of oxygen (pO_2) in healthy human tissues is around 3-6% (30, 31), but within lymphoid tissues, distinctive hypoxic regions exist (pO_2 ~0.5-1%), as specifically observed in GC light zone regions (32–34). However, the role of variations in pO_2 on human B cell differentiation, and fate decision into memory B cells and antibody secreting cells has not been studied. In fact, the vast majority of *in vitro* studies is carried out at atmospheric oxygen levels ((pO_2 ~21%), which is much higher than proliferating B cells will encounter *in vivo*.

Variations in pO_2 are likely to affect the amplitude of B cell differentiation, due to profound effects of cellular metabolism as well as direct effects on transcriptional regulation (30, 31, 35–38). Although, contrasting findings have been reported for the influence of hypoxia on GC responses in mice, negative

effects on class switch recombination and proliferation are repeatedly described (32, 34, 39). Others observed increased Tfh function induced by upregulation of HIF-1α, a major transcription factor involved in the cellular sensing of pO_2 (33). Not all previous studies have been able to confirm HIF-1α expression within GC B cells, suggesting hypoxia may regulate B cell function independent of HIF-1α (40). Another study comparing hypoxic (1%) and venous (5%) pO_2 reported decreased class switch recombination and altered cellular metabolism upon culture at hypoxic pO_2 (32). Overall, oxygen pressure appears an important but as yet poorly understood variable in B cell differentiation.

In the present study, we systematically investigated the effect of atmospheric (21%), normoxic, tissue-associated (3%), and hypoxic (1%) pO_2 on human B cell differentiation in our highly optimized system for human primary B cell culture. Moreover, in line with varying oxygen pressures during B cell cycling in the GC dark zone and light zone, we studied time-dependent transitions in pO_2 during culture and its effects on B cell differentiation trajectories and IgG class switch recombination. We show that different oxygen pressures distinctly regulate human naive B cell differentiation and class switch recombination.

Results

Differential pO_2 controls human B cell differentiation into CD27$^+$ and antibody secreting cell compartments

The contribution of pO_2 on human naive B cell differentiation was investigated in B cell differentiation cultures while maintaining constant pCO_2. Resting naive B cells (CD19$^+$IgD$^+$CD27$^-$IgG$^-$IgA$^-$) from human peripheral blood were stimulated under atmospheric ($pO_2 = 21\%$), normoxic ($pO_2 = 3\%$) or hypoxic ($pO_2 = 1\%$) conditions, using a combination of CD40L-expressing 3T3 cells (12), IL-4 and IL-21, known to facilitate class switch recombination, memory B cell and antibody secreting cell formation (Figure 1A) (12, 41, 42). Alterations in pO_2 did not affect CD40L expression levels on 3T3 cells used for stimulation (Figure S2I, subtype high). Up until day 7 B cell survival was similar among pO_2 conditions, but at day 11 hypoxic cultures contained fewer cells (Figures S2A,B). In all cultures a rapid upregulation of activation marker CD80 was observed (Figure S2C). Remarkably, naive B cell differentiation, as determined by the formation of antibody secreting cells (CD27$^+$CD38$^+$) and CD27$^+$ (CD27$^+$CD38$^-$) B cells, was dramatically altered by differential pO_2. Hypoxia induced a 5 to 10-fold induction of CD27$^+$ B cells as compared to atmospheric (p<0.0001) and normoxic cultures (p<0.0001) at day 7 (Figures 1B, C), and absolute cell no. in Figure S2D), at the expense of antibody secreting cell formation at day 11. In addition,
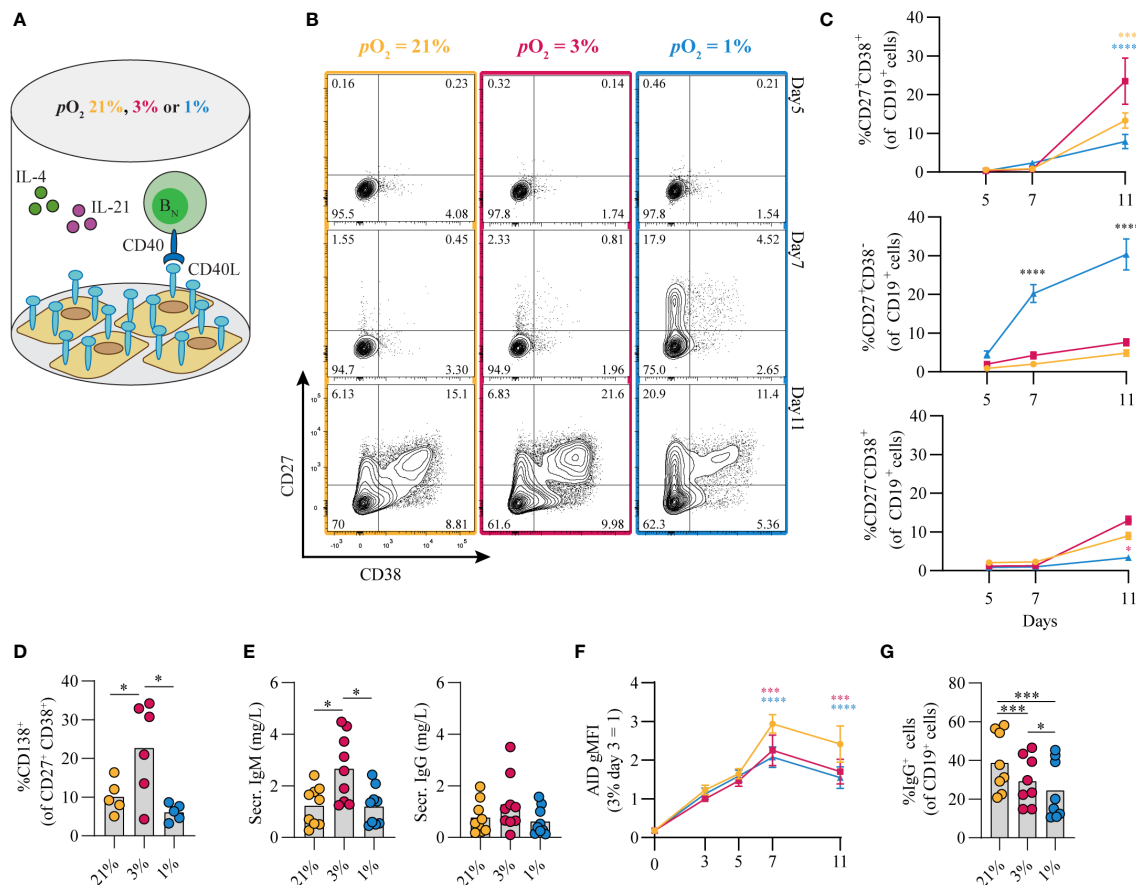
FIGURE 1

Differential pO_2 controls human B cell differentiation into $CD27^+$ and antibody secreting cell compartments. **(A)** Schematic overview of B cell *in vitro* culture system. 250 resting human naive B cells ($CD19^+CD27^-IgD^+$) were stimulated using a human CD40L-expressing feeder cell layer (subtype 'High' (12),); recombinant human IL-4 (25ng/ml) and IL-21 (50ng/ml); and cultured at 5% pCO_2 and 21, 3, or 1% pO_2 for a maximum of 11 days. **(B)** Representative biaxial CD27/CD38 FACS plots after 5, 7, and 11 days of culture at 21, 3, or 1% pO_2. **(C)** Quantification of the percentages of CD27 and CD38 subpopulations within total $CD19^+$ B cells over time ($n = 9$). **(D)** CD138 expression within the $CD27^+CD38^+$ antibody secreting cell population ($n = 6$). **(E)** Cumulative secretion of IgM and IgG measured in culture supernatants after 11 days ($n = 9$). **(F)** gMFI of AID expression over time ($n = 3$). **(G)** Percentage of IgG^+ cells within $CD19^+$ B cells, combined surface and intracellular staining ($n = 8$). Bars represent means of biological replicates each composed of 2 technical replicates in **(D, F)** 2, **(E, G)** 3 or **(C)** 4 independent experiments. Statistical differences were determined using **(C, F)** mixed-effects analysis using Tukey's test for multiple comparisons **(D, E, G)** repeated measures one-way ANOVA using Tukey's test for multiple comparisons. *p < 0.05, ***p < 0.001, ****p < 0.0001.
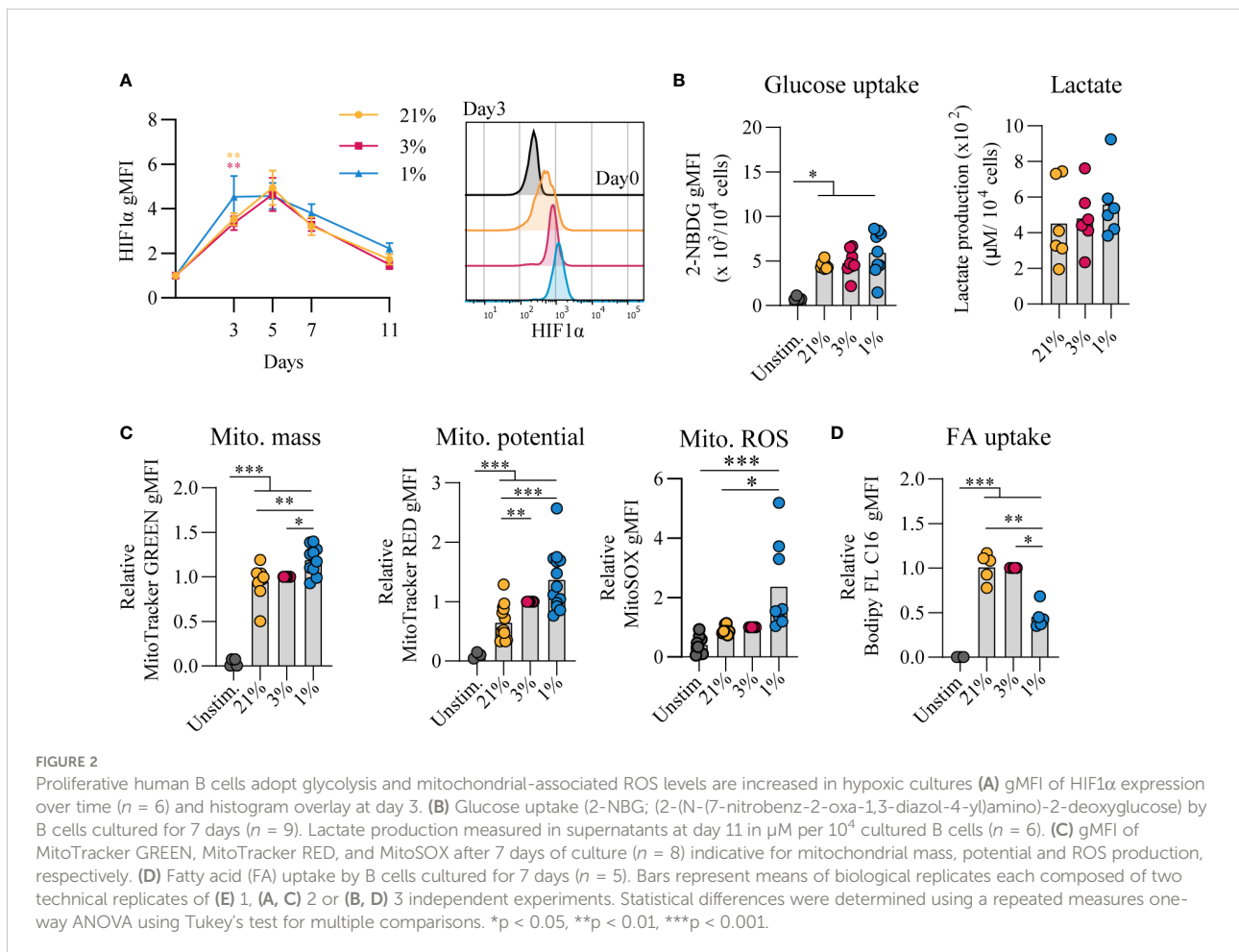
in normoxic cultures, the relative numbers of $CD138^+$ antibody secreting cells were 2 to 4-fold increased relative to atmospheric (p<0.001) and hypoxic cultures (p<0.0001, Figure 1D), in line with increased concentration of secreted IgM and IgG in normoxic culture supernatant at day 11 (Figure 1E). Naive B cells poorly survived and differentiated when cultured under extreme hypoxic conditions (pO_2 = 0.5%, Figure S2E, F). Furthermore, using 3T3 cells with higher or lower expression of CD40L resulted in reduced proliferation, especially at reduced oxygen pressures (resp. 'VH', and 'Low', vs 'High'; Figures S2H, I). The addition of anti-IgM F (ab')$_2$s to the cultures, as additional BCR stimulation, did not alter *in vitro* B cell survival and differentiation at differential pO_2s (Figure S2J). Next, we assessed the effect of pO_2 on antibody class switching and Ig production. Protein expression of DNA-editing

enzyme AID –indispensable for class switch recombination and somatic hypermutation– were substantially elevated over time regardless of oxygen pressure, but significantly lower at low pO_2 at day 7 and 11 (Figure 1F), in accordance with previous studies in mice (32), reflecting the overall larger fraction of differentiated cells under these conditions (Figures 1B, C, S2K). In line with AID expression levels, IgG^+ B cell frequencies were higher in atmospheric cultures (p<0.001, Figure 1F) with minimal switch to IgA^+ overall, as was expected by the IgG promoting culture conditions (CD40L + IL-21 + IL-4, Figure S2L). Altogether, these data illustrate a profound regulation of human naive B cell differentiation by oxygen levels and show that normoxia promotes differentiation into potent antibody secreting cells while hypoxia promotes differentiation into $CD27^+$ B cells.

Proliferative human B cells adopt glycolysis and mitochondrial-associated ROS levels are increased in hypoxic cultures

Given that cellular metabolism has been reported to be linked to gene expression and B cell differentiation (43), we assessed the metabolic status of B cells that were cultured at different pO_2s. Using flow cytometry, HIF1α levels were increased throughout hypoxic cultures compared to normoxic and atmospheric cultures (Figure 2A). After 7 days of *in vitro* stimulation B cells showed similar increase in cell size in all conditions compared to unstimulated cells (Figure S3A). Dividing lymphocytes typically rely on aerobic glycolysis, fermenting imported glucose into lactate rather than oxidizing it in the mitochondria for energy. Glycolytic activity was assessed by uptake of 2-NBDG, a fluorescent analog of glucose, and production of lactate as an end product of glycolysis. Uptake of 2-NBDG and lactate production were not significantly different between different

pO_2 culture conditions, but overall higher compared to resting naive B cells suggesting that indeed stimulated B cells require more glucose but demands did not change considerably upon differential pO_2 environments (Figure 2B). Also expression of GLUT1, a glucose transporter, varied minimally between culture conditions (Figure S3B). To asses mitochondrial oxidative metabolism we analyzed mitochondrial mass, potential and formation of reactive oxygen species (ROS) by flow cytometry at day 7. Mitochondrial mass, potential and mitochondrial ROS were higher in B cells cultured at hypoxic conditions (Figure 2C). Uptake of a fluorescent fatty acid probe was reduced in B cells under hypoxic conditions (Figure 2D), suggesting these cells rely less on oxidation of fatty acids. At day 11 metabolic markers yielded similar result among different pO_2 conditions, except for ROS levels that were significantly higher in hypoxic cultures compared to atmospheric cultures (Figure S3C). Taken together, these results indicate that highly proliferative B cells adopt glycolysis independent of local pO_2 levels and mitochondrial-associated ROS levels are elevated in hypoxic cultures.

FIGURE 2

Proliferative human B cells adopt glycolysis and mitochondrial-associated ROS levels are increased in hypoxic cultures **(A)** gMFI of HIF1α expression over time (*n* = 6) and histogram overlay at day 3. **(B)** Glucose uptake (2-NBG; (2-(N-(7-nitrobenz-2-oxa-1,3-diazol-4-yl)amino)-2-deoxyglucose) by B cells cultured for 7 days (*n* = 9). Lactate production measured in supernatants at day 11 in μM per 10^4 cultured B cells (*n* = 6). **(C)** gMFI of MitoTracker GREEN, MitoTracker RED, and MitoSOX after 7 days of culture (*n* = 8) indicative for mitochondrial mass, potential and ROS production, respectively. **(D)** Fatty acid (FA) uptake by B cells cultured for 7 days (*n* = 5). Bars represent means of biological replicates each composed of two technical replicates of **(E)** 1, **(A, C)** 2 or **(B, D)** 3 independent experiments. Statistical differences were determined using a repeated measures one-way ANOVA using Tukey's test for multiple comparisons. *$p < 0.05$, **$p < 0.01$, ***$p < 0.001$.

pO_2 steers canonical signaling pathways that direct naive B cell differentiation pathways

The amplitude of B cell proliferation and differentiation is regulated by a complex interplay of signaling pathways induced by antigen recognition, CD40 ligation and reception of Tfh-derived cytokines IL-4 and IL-21 (summarized in Figure S4A) (8, 44). Upregulation of BCL6 as well as IRF4 expression

suggests differentiation of cells with a GC-like phenotype (Figures 3A, B, respectively). In line, PNA positivity, indicative for expression of GC-specific glycans, and CD95 expression was observed early on in culture and decreased prior to the generation of CD27$^+$ B cells and antibody secreting cells (Figures 3C, D). PNA binding was reduced for B cells cultured at hypoxic pO_2 at day 3 and 5 potentially due to the accelerated CD27$^+$ differentiation in hypoxic cultures. Expression of CD86, an activation marker highly expressed
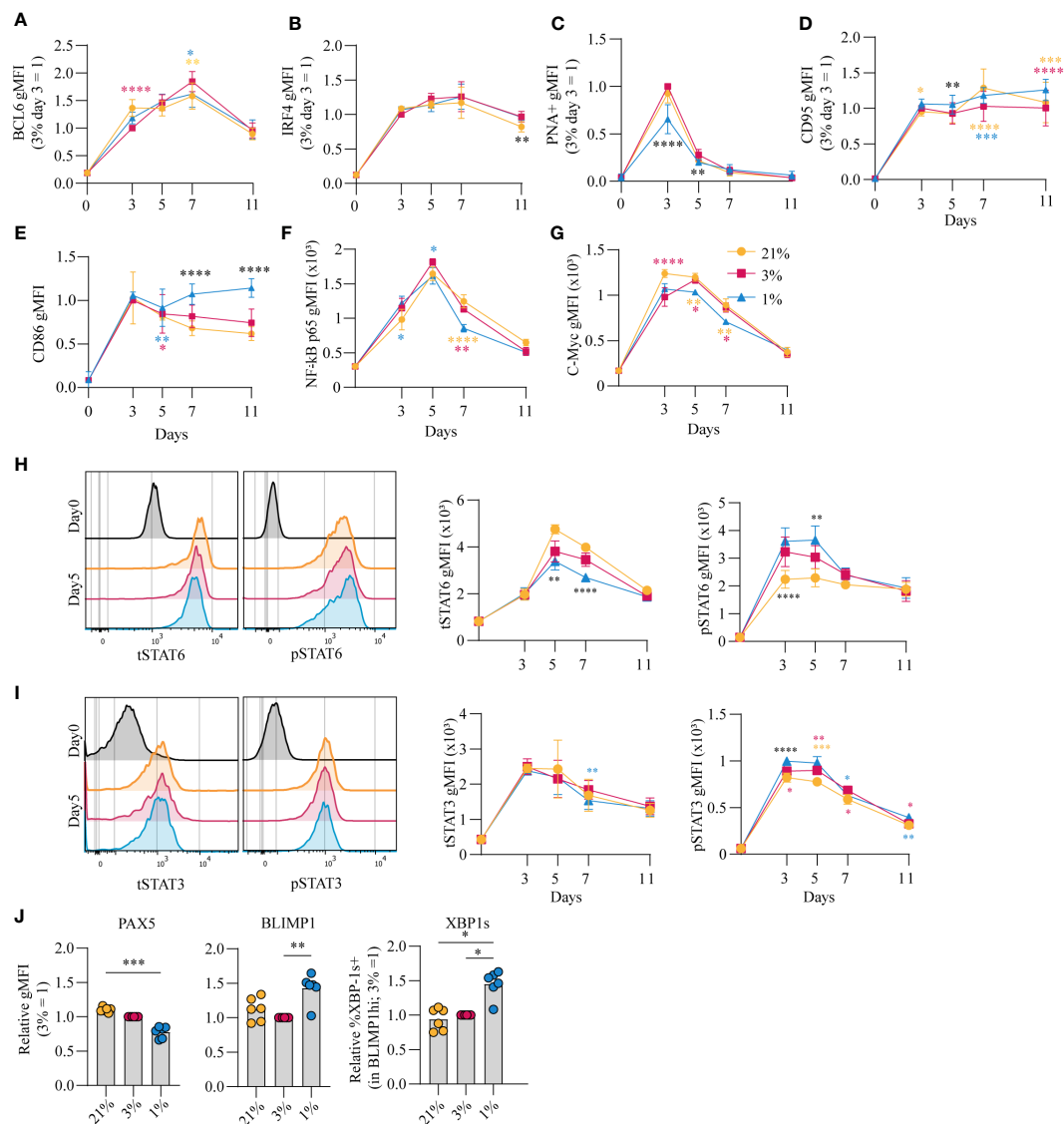

FIGURE 3

pO_2 steers canonical signaling pathways that direct naive B cell differentiation pathways **(A-D)** gMFI of **(A)** BCL-6 (*n* = 6) **(B)** IRF4 (*n* = 6) **(C)** PNA+ (*n* = 6) **(D)** CD95 (*n* = 6) **(E)** CD86 (*n* = 6) **(F)** NFκB active subunit p65 (*n* = 9) **(G)** c-Myc (*n* = 9) **(H-I)** gMFI of **(H)** tSTAT6 and pSTAT6 and **(I)** tSTAT3 and pSTAT3 over time in culture (*n* = 6) and (left panels) representative histogram overlays of pSTAT and tSTAT expression on day 5 of culture **(J)** gMFI of PAX5, BLIMP1 and %XBP-1s+ in BLIMP1hi cells (n=6) on day 7 **(A-J)** Bars represent means of biological replicates each composed of two technical replicates of 2 **(H-J)** or **(A-G)** 3 independent experiments **(A-I)** Differences in gMFI were determined using mixed-effects analysis using Tukey's test for multiple comparisons. **(J)** Differences in gMFI were determined using repeated measures one-way ANOVA using Tukey's tests for multiple comparisons. *p < 0.05, **p < 0.01, ***p < 0.001, ****p < 0.0001.

on light zone B cells ([45](#), [46](#)), increased rapidly during culture and remained significantly higher expressed on B cells cultured at hypoxic pO_2 (Figure 3E). CD40 signaling primarily shapes the magnitude of B cell expansion and survival through induction of NFκB p65 and c-Myc ([21–23](#)). Moreover, NFκB p65 and c-Myc are reported to maintain cellular GC commitment ([47](#)). B cells cultured at hypoxic pO_2 showed a reduction in NFκB p65 (Figure 3F) and c-Myc (Figure 3G) expression from day 5 onwards, supporting the concomitant differentiation into CD27$^+$ cells, and to a lesser extent antibody secreting cells, at day 7 and reduced B cells numbers observed in hypoxic cultures thereafter (Figure S2B).

Next, the effect of pO_2 on the IL-4R/IL-21R signaling pathways to regulate B cell and antibody secreting cell transcriptional programs was analyzed. Increased phosphorylation of STAT6 (pSTAT6), a signaling protein downstream of the IL-4R, was observed in B cells cultured at hypoxic pO_2, peaking at day 3 and 5 ($p < 0.01$ at day 5) (Figure 3H, S4B). This coincided with higher expression of XBP-1s, a transcription factor (TF) downstream of pSTAT6, at day 7 (Figure 3J, right panel), and was not the result of variable IL-4R expression levels, determined by RT-qPCR (Figure S4C). Peak levels of pSTAT3 on day 3 and 5, with minor differences when comparing the different pO2 conditions (Figure 3I, S4D), coincided with upregulation of BLIMP1, directly downstream of pSTAT3, and repression of PAX5, most prominently in B cells cultured at hypoxic pO2 (Figure 3J, S4E). PAX5 supports B cell identity. Consistent with this activity, B cells cultured at atmospheric pO2 retained highest PAX5 levels throughout culture, and thus overall a lower fraction of differentiated cells under this conditions (Figure 3I, S4D) ([48](#)). Expression of BLIMP1 and XBP-1s was higher under hypoxic conditions (Figure 3J), and did not differ within the CD27$^-$CD38$^-$ population at varying pO_2 at day 7 (Figure S4F), suggesting elevated BLIMP1 and XBP-1s expression in B cells cultured at hypoxic pO_2 arises from the expanded CD27$^+$ compartment (Figure 1C). This CD27$^+$ population did not secrete more Ig at day 7 compared to cells cultured at normoxic or atmospheric pO_2 despite elevated XBP-1s expression, which is essential for the unfolded protein response in antibody secreting cells (Figure S4G). At day 11, naive B cells differentiation into antibody secreting cells in normoxic cultures outperformed atmospheric cultures in which B cells retained higher PAX5 levels and repression of BLIMP1 and XBP-1s (Figure S4H). Furthermore, cells in normoxic cultures had highest XBP-1s levels in line with higher Ig production observed in these cultures ($p < 0.05$) (Figure 1G). Overall, B cell culture at different pO_2 affects CD40-, IL-21R- and IL-4R-dependent signaling pathways essential for efficient B cell survival and differentiation. Expression dynamics of B differentiation-associated TFs PAX5, BLIMP1 and XBP1 were influenced by local pO_2, skewing the formation of CD27$^+$ and/or antibody secreting cell populations at hypoxic or normoxic pO_2, respectively.

Hypoxic pO_2 drives generation of a unique CD27^{++} B cell population, with enhanced antibody secreting cell differentiation capacity and Ig production upon restimulation

Culturing B cells at hypoxic pO_2 resulted in a remarkable increase in CD27$^+$ B cells which emerged earlier as compared to atmospheric and normoxic cultures (Figure 1C). Interestingly, there was not only enlargement of this compartment but also formation of a population of CD27^{++} cells (4.4% of CD19+ population), absent in normoxic and atmospheric cultures at day 7 ($p < 0.05$) (Figure 4A, S5) To assess the phenotype of these CD27^{++} B cells, transcription factor profiles directing B cell differentiation were compared between CD27$^-$, CD27$^{+/-}$, CD27$^{+/+}$ and CD27^{++}CD38^{++} populations that developed under hypoxic pO_2 at day 7 (Figure 4B). PAX5 expression was lower and BLIMP1 expression higher in CD27$^{+/++}$ cells compared to CD27$^-$CD38$^-$ B cells, with PAX5 and BLIMP1 expression being similar between CD27^{++} and CD27^{++}CD38^{++} populations (Figure 4C, upper and middle panel). Expression of XBP-1s increased as differentiation progressed, being highest in the CD27^{++}CD38^{++} population (Figure 4C, lower panel). Moreover, a rise in the frequency of IgG$^+$ B cells coincided with increasing CD27 expression, being highest in the CD27^{++} population (Figure 4D).

As the CD27^{++} showed a distinct transcriptional profile compared to CD27$^{+/-}$ and CD27$^-$ B cells, we assessed whether this translated into functional differences with regard to antibody secreting cell differentiation and Ig production. To this end naive B cells were cultured for 7 days under hypoxia, after which different CD27 expressing populations were sorted and subsequently cultured at antibody secreting cell-promoting normoxic pO_2 for an additional 4 or 7 days (Figure 4E). CD27^{++} cells showed a significant increase in antibody secreting cell differentiation and antibody production as compared to the CD27$^{+/-}$ and CD27$^-$ subsets ($p < 0.05$) (Figure 4F), indicating that with the same level of stimulation the CD27^{++} cells had enhanced capacity to differentiate towards functional antibody secreting cells. In summary, a population of CD27^{++} B cells emerged exclusively in hypoxic cultures, with the potential to rapidly differentiate into antibody secreting cells and produce Ig after restimulation.

Time-dependent pO_2 transitions alter B cell differentiation dynamics and promote class switch recombination to IgG

Given that during an *in vivo* GC reaction B cells cycle between the hypoxic light zone and normoxic dark zone, we assessed the effect of a pO_2 transition on B cell differentiation
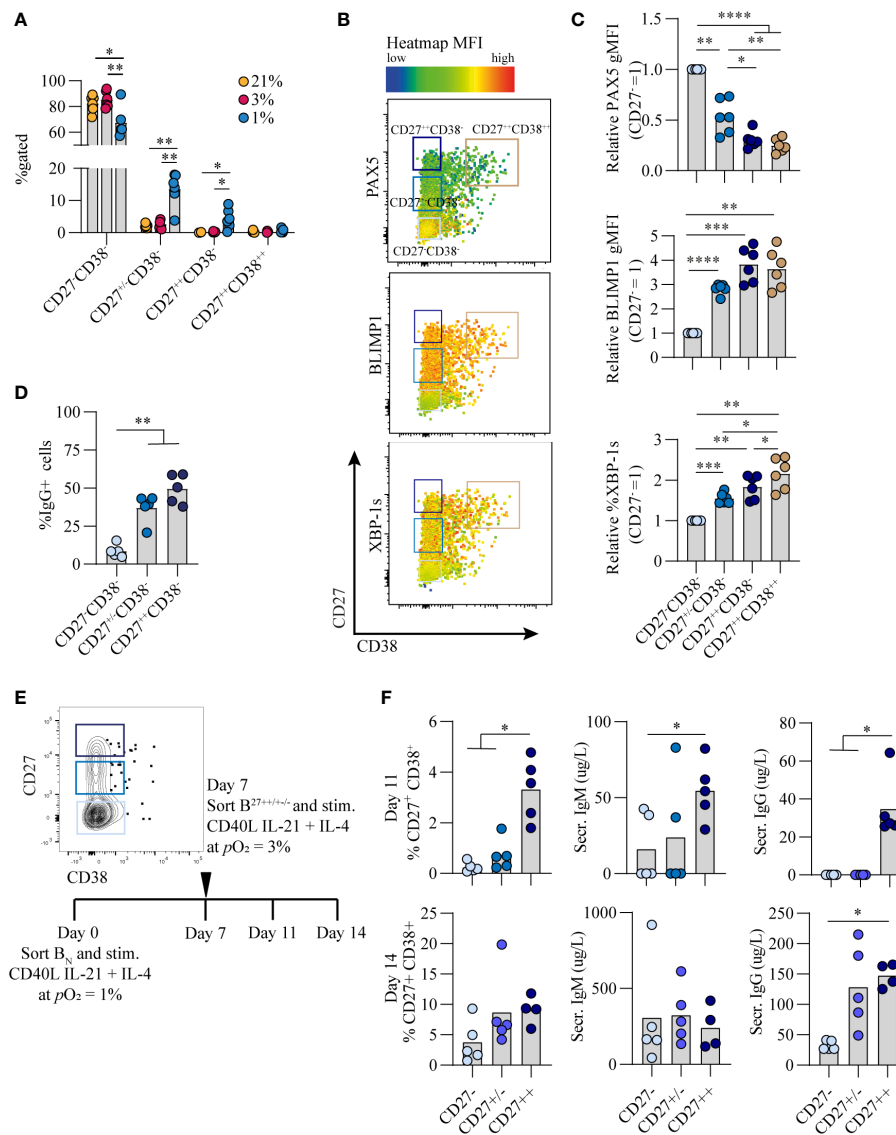
FIGURE 4

Hypoxic pO_2 drives generation of a unique CD27++ B cell population, with enhanced antibody secreting cell differentiation capacity and Ig production upon restimulation **(A)** Quantification of percentage of CD27-CD38-, CD27+/-CD38-, CD27++CD38- and CD27++CD38++ cells on day 7 of culture (n = 5) **(B)** Representative biaxial flow cytometry plot of CD27 and CD38 expression, with heatmap depicting MFI expression of PAX5, BLIMP1 and XBP-1s on day 7. **(C)** gMFI of PAX5, BLIMP1 and XBP-1s in respective populations of CD27-CD38-, CD27+/-CD38-, CD27++CD38- and CD27++CD38++ cells on day 7 (n = 6) **(D)** Percentage of IgG+ B cells on day 7 of of culture at 1% pO2 within CD27++ CD38-, CD27+/- CD38- or CD27- CD38- populations. (n = 5) **(E)** Representative example of FACS sort gating strategy on day 7 to isolate CD27++ CD38-, CD27+/- CD38- or CD27- CD38- B cells with schematic experimental time line. **(F)** Quantification of %CD27+CD38+ cells by flow cytometry and IgG and IgM secretion by ELISA, 4 or 7 days after sort (day 11 or 14 of culture) (n = 5). **(A-F)** Bars represent means of biological replicates each composed of two technical replicates of **(A, C, D)** 2 or **(F)** 1 independent experiment **(A)** Differences in %gated cells were determined using mixed-effects analysis using Tukey's test for multiple comparisons. **(C, D, F)** Differences in gMFI and % gated cells were determined using repeated measures one-way ANOVA using Tukey's test for multiple comparisons. *p < 0.05, **p < 0.01, ***p < 0.001, ****p < 0.0001.

and class switch recombination *in vitro*. To this end, naive B cells were cultured at either hypoxic or normoxic pO_2 and transferred at stated time points to normoxic or hypoxic pO_2, respectively. Independent of timing, a transition from hypoxic to normoxic pO_2 increased antibody secreting cell differentiation concomitant

with decreased CD27+ cell formation (Figures 5A, B). Transition from hypoxic to normoxic pO_2 at day 3 of culture enhanced antibody secreting cell differentiation at day 11 compared to continued culture at hypoxic pO_2 and was similar to continuous culture under normoxic pO_2 (Figures 5A, B),
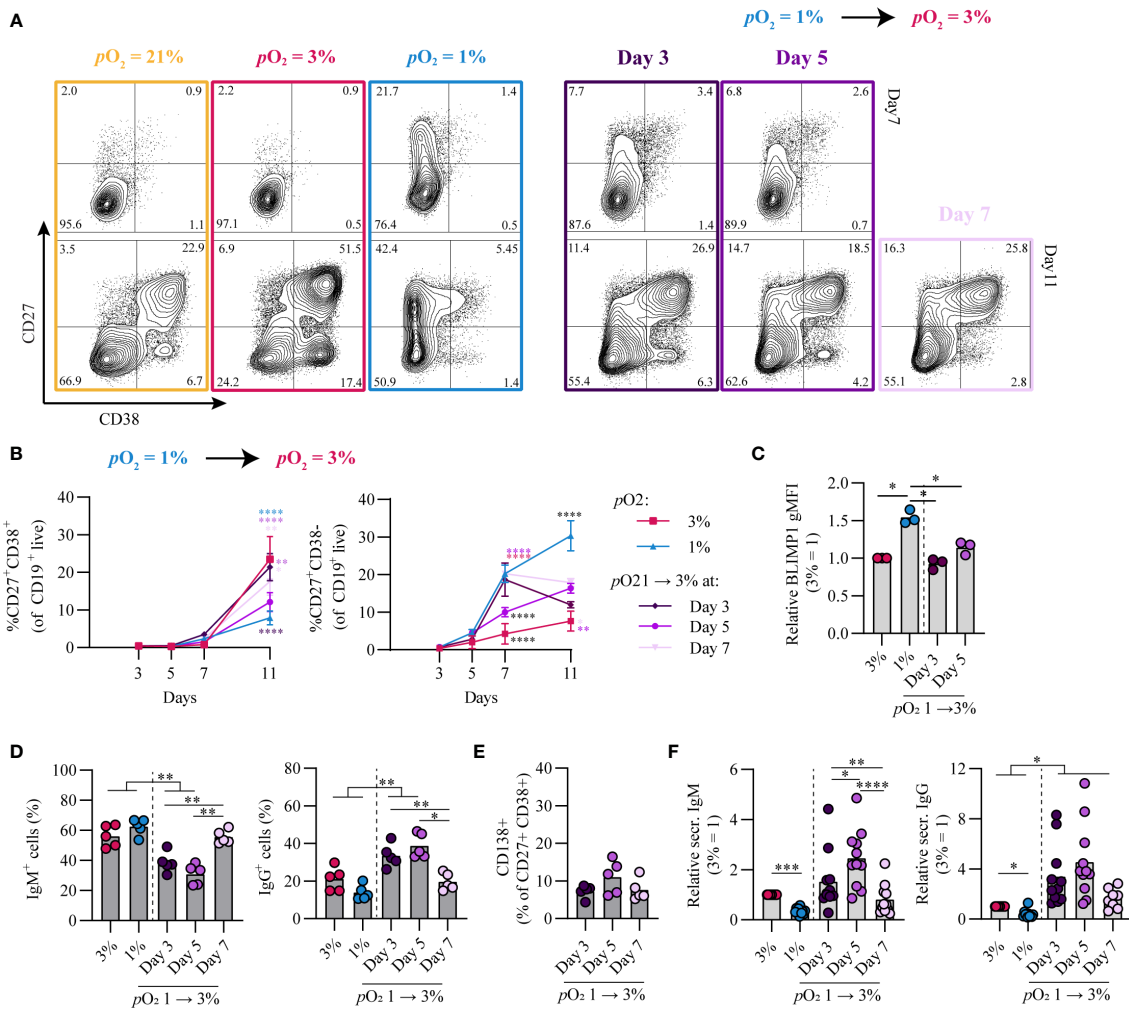
FIGURE 5

Time-dependent pO_2 transitions alter naive B cell differentiation and IgG class switch recombination. **(A)** Representative biaxial CD27/CD38 FACS plots of 21, 3, 1% pO2 cultures and $1 - 3\%$ pO_2 transition cultures at day 3, 5 or 7 shown for day 7 and 11 of culture. **(B)** Quantification of CD27+CD38+ and CD27+CD38- B cells over time in culture ($n = 11$) **(C)** gMFI of BLIMP1 on day 7 ($n = 3$) **(D)** Frequency of IgM+ and IgG+ B cells on day 11 ($n = 5$). **(E)** CD138 expression within the CD27+CD38+ population ($n = 5$). **(F)** IgM and IgG levels were measured by ELISA in culture supernantant after 11 days ($n = 11$). Bars represent means of biological replicates each composed of two technical replicates of **(B, F)** 3, **(D)** 2 or **(C, E)** 1 independent experiment. **(B)** Statistical differences were determined using mixed-effects analysis using Tukey's test for multiple comparisons **(C-F)** Differences in gMFI, % gated cells and Ig production were determined using repeated measures one-way ANOVA using Tukey's test for multiple comparisons. *$p < 0.05$, **$p < 0.01$, ***$p < 0.001$, ****$p < 0.0001$.

with BLIMP1 expression lower compared to hypoxic cultures and similar to levels observed in normoxic cultures (Figure 5C). A transition from 1 to 3% pO_2 at day 5 led to a moderate generation of CD27+ B cells and reduced antibody secreting cells formation in line with continuous hypoxic cultures. When hypoxic cultures were transitioned to normoxic pO2 at day 7, this induced an efficient formation of antibody secreting cells at day 11. Different from cultures at hypoxic pO_2 on day 3 and 5, at day 7 hypoxic cultures consist for a significant proportion (~20%) of CD27+/++ B cells, which efficiently differentiate to antibody secreting cells upon

restimulation and transition to normoxic pO_2 as was shown in Figure 4F. Overall this suggests time-dependent transitions in pO_2 steer B cell differentiation, where early (day 3) transitions from hypoxic to normoxic pO_2 lead to antibody secreting cell formation comparable to continuous normoxic cultures whereas a pO_2 transition later on during culture (day 7) induces antibody secreting cell formation - in part - via the CD27++ compartment. These data show that *in vitro* B cell differentiation can occur *via* distinct trajectories steered by differential pO_2, where hypoxia drives differentiation *via* a CD27++ population and atmospheric and normoxic pO_2 *via* CD38+ or directly

towards antibody secreting cells (Figure S6A). Remarkably, transitions from hypoxic to normoxic pO_2 at day 3 and 5 enhanced class switch recombination to IgG$^+$ B cells concomitant with a reduction in IgM$^+$ B cells (Figure 5D). Even though the percentage of CD138$^+$ antibody secreting cells was similar (Figure 5E) and lower compared to continuous normoxic cultures (Figure 1D), transition of hypoxic to normoxic pO_2 at day 3 and 5 resulted in higher quantities of secreted IgM and IgG in culture supernatants (Figure 5F). Enhanced IgG class switch recombination and Ig production were no longer observed when the pO_2 transition was made at day 7.

Vice versa, transition from normoxic to hypoxic pO_2 at day 3 and 5 enhanced CD27$^+$ B cell formation and BLIMP1 expression compared to continuous normoxic cultures and was more similar to continuous hypoxic cultures (Figures S6B–D). A transition at day 7 from normoxic to hypoxic pO_2 was deleterious for both CD27$^+$ B cell and antibody secreting cell differentiation. class switch recombination to IgG$^+$ B cells and Ig production levels ranged between those found in continuous normoxic and hypoxic cultures (Figures S6E–G).

Overall, time-dependent transitions between hypoxic and normoxic pO_2 during culture govern different human B cell differentiation trajectories and IgG class switch recombination *in vitro*.

Discussion

The GC reaction is at the heart of the humoral immune response. Both extrafollicular and GC B cell responses take place within human tissues where oxygen pressure may range from 0.5-6% pO_2 with hypoxic regions (0.5-1% pO_2) described within GC light zone regions. Preciously little information is available about the potential role of local pO_2 on human B cell fate decision during their cycling between dark zone and light zone, typically characterized by dissimilar oxygen pressures. Here we studied the effect of atmospheric (21%), tissue associated (normoxia, 3%) and hypoxic (1%) pO_2 on human B cell differentiation. We observe profound differences in B cell differentiation, dynamics of emergence of various cell populations, class switch, and Ig production under these different oxygen pressures. Figure 6 summarizes our key findings on the contribution of pO_2 on human naive B cell differentiation. In both hypoxic and normoxic cultures, naive B cells differentiated into a GC-like phenotype as evidenced by the expression of BCL6 and IRF4, as well as increased expression of CD95 and PNA binding. Similar to light zone B cell phenotype and function *in vivo* (8), B cells cultured at hypoxic pO_2 showed high expression of CD86 and differentiated rapidly into CD27$^+$ B cells. Moreover, culture at hypoxic pO_2 generated a unique population of CD27^{++} B cells efficient in antibody secreting cell differentiation and Ig production upon restimulation. In

normoxic cultures, naive B cells predominantly differentiated into antibody secreting cells, which occurred less rapidly compared to CD27$^+$ B cell formation at hypoxic pO_2 in line with time-dependent waves of memory B cell and antibody secreting cell formation *in vivo* (2). Finally, time-dependent transitions from hypoxic to normoxic pO_2 during culture changes B cell differentiation trajectories and promotes IgG class switch recombination and Ig production. This indicates during *in vivo* B cell cycling between GC light zone and GC dark zone, the dynamic variation in pO_2 is also likely to form another regulatory layer for human B cell differentiation. Overall, our results identify oxygen as a critical factor in dictating human B cell differentiation and demonstrate the necessity of incorporating GC-like physiological pO_2 variations rather than continuous atmospheric pO_2 to study human B cell responses *in vitro*.

In vivo, antigen-specific triggering of the BCR is required for the generation of an efficient GC response. We did not observe an effect on B cell survival or differentiation by addition of a BCR stimulus to the B cell cultures at different pO_2, in line with previous reports showing limited additional effects of BCR triggers in *in vitro* cultures (12). Despite the absence of a BCR trigger, we saw a clear upregulation of c-Myc expression which is normally upregulated upon positive selection in the GC, in line with previous reports indicating CD40L ligation to be sufficient to induce c-Myc expression (25). We observed a reduction of c-Myc and NFκB expression in cells cultured at hypoxic pO_2 after an initial surge upon culture initiation. c-Myc and NFκB signaling play a major role in transcriptional regulation of GC B cell proliferation and cell survival, thereby correlating with our observations regarding reduced cell numbers towards the end of cultures at hypoxic pO_2. Naive B cell survival was abrogated upon culture at 0.5% pO_2 and upon higher CD40L co-stimulation (subtype VH) at low pO_2, but not atmospheric pO_2, due to impaired proliferation. Hence, the level of CD40L co-stimulation impacts B cell survival at physiological pO_2.

Highly proliferative lymphocytes have been described to adopt glycolysis (49), which -although not comprehensively studied- is in line with the increase in glycolysis-associated metabolic traits observed in our cultures independent of *in vitro* pO_2. B cells cultured under hypoxic pO_2 carried out mitochondrial oxidative metabolism, in addition to glycolysis. The difference in B cell differentiation trajectories and expansion of the CD27$^+$ compartment in hypoxic cultures may explain the expanded metabolic program towards mitochondrial oxidative metabolism at day 7. Much of the research on crosstalk between immune responses and pO_2 has focused on the TF HIF1α. We observe upregulation of HIF1α expression throughout all culture conditions not only at hypoxic pO_2. HIF1α can also be induced by signaling through CD40L, BCRs as well as TLR ligands, probably explaining the increase in HIF1α also in non-hypoxic cultures (50). Furthermore, a recent study could not identify
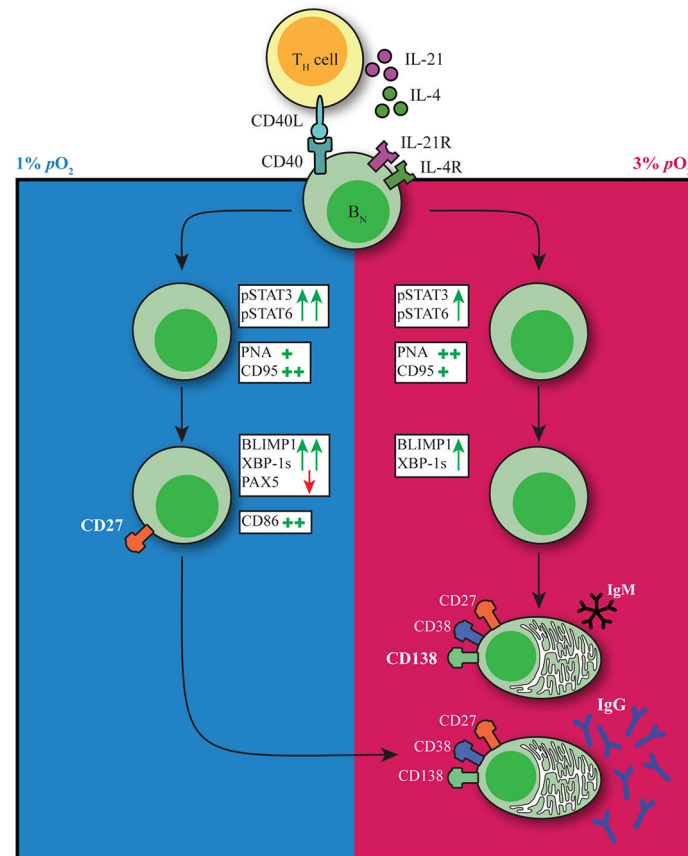
FIGURE 6

pO_2 as a critical driver of B cell differentiation *in vitro*. Schematic representation of the effect of differential pO_2 on B cell differentiation and underlying signaling pathways.

expression of hypoxia-induced genes in *ex vivo* analyzed mouse GC B cells (40), indicating HIF1α is not the sole regulator of hypoxia-associated responses.

Clear differences were observed in the expansion of CD27$^+$ B cell and/or antibody secreting cell compartments in human naive B cells cultures at hypoxic and normoxic pO_2, respectively, driven by differences in the underlying molecular pathways regulating B cell survival and differentiation. It has been shown that there is a time-dependent developmental switch in the output of the GCs, such that it first dedicates itself to memory B cell generation and later switches to mainly producing antibody secreting cells (2). During culture of naive B cells at hypoxic pO_2 a hypoxia-dependent CD27^{++} population emerged early during culture. The question arises whether these CD27^{++} cells may resemble memory B cell generated early within a GC response. Albeit unanswered in this study, it did become clear that these CD27^{++} cells did not secrete Igs, whereas upon restimulation they swiftly differentiated into antibody secreting cells and exhibited efficient Ig secretion, in line with

functionalities of memory B cells (51). Nevertheless, these cells clearly expressed a transcription factor signature of increased BLIMP1 and XBP-1s expression concomitant with a reduction of the B cell identity TF PAX5, similar to antibody secreting cells and different from memory B cells (16, 19). In line with varying pO_2 during a GC response, where B cells cycle between hypoxic light zone to normoxic dark zone, we observed time-dependent effects of pO_2 transitions on human B cell differentiation trajectories. Taken together, hypoxic pO_2 primes B cells for efficient antibody secreting cell differentiation from a CD27$^+$ phenotype that, in order to occur, favors a transition to a normoxic environment. Besides B cell differentiation trajectories, also IgG class switch recombination was influenced by pO_2 transitions. When cultured at continuous pO_2, atmospheric pO_2 yielded the highest proportion of IgG$^+$ B cells (albeit not corroborated with equally elevated levels of IgG antibody production). Similar numbers of IgG$^+$ B cells could be generated in cultures that transitioned from hypoxic to normoxic pO_2 at day 3 or 5. Overall, our *in vitro* studies

demonstrate the necessity of incorporating GC-like physiological pO_2 variations rather than continuous atmospheric pO_2 to study human B cell responses *in vitro*, as it more closely resembles the *in vivo* GC microenvironment and recapitulates time-dependent regulation of B cell fate decisions.

Besides local pO_2, other factors such as availability of nutrients, migratory and physical signals such as shear stress are also likely to contribute to B cell fate decision during both extrafollicular and GC B cell responses, warranting the need for 3D culture systems or organoids that more closely resemble the GC microenvironment to facilitate human *in vitro* B cell differentiation studies. In addition, several pathological conditions have been described to be related to hypoxia, such as myocardial ischemia (52), metabolic diseases (53), chronic heart and kidney diseases (54), and reproductive diseases (55). Moreover, pO_2 has been measured and found to be significantly reduced in the majority of tumors, and sensitivity to chemotherapeutic agents changed dramatically under hypoxic conditions (56–58), highlighting the importance to adopt hypoxic cultures also for other avenues such as cancer-related drug testing and *in vitro* disease models.

In summary, we demonstrate that oxygen is an important regulator of human naive B cell differentiation by promoting oxygen-dependent differentiation trajectories and IgG class switch recombination.

Materials and methods

Isolation of human naive B cells

Buffy coats were obtained from anonymized healthy donors with written informed consent in accordance to the guidelines established by the Sanquin Medical Ethical Committee and in line with the Declaration of Helsinki. Human Peripheral blood mononucleated cells (PBMCs) were isolated from fresh buffy coats using Ficoll gradient centrifugation (lymphoprep; Axis-Shield PoC AS). CD19^{+} cells were isolated by positive selection using magnetic Dynabeads (Invitrogen). Cryopreserved CD19^{+} cells were resuspended in PBA (PBS supplemented with 0.1% bovine serum albumin) and stained for surface markers 30 minutes in the dark at 4°C. Viable, singlet naive B cells (CD19^{+}IgD^{+} CD27^{-}IgG^{-}IgA^{-}) were sorted on a FACS Aria II/III.

Human B cell cultures

3T3 mouse fibroblast cells expressing human CD40L (subtype: high), described previously (12), were harvested and irradiated with 30 Gy and seeded $10x10^3$ cells/well on 96-well plates for overnight adherence in B cell culture medium (RPMI

medium supplemented with FCS (5%, Bodinco), penicillin (100 U/mL, Invitrogen), streptomycin (100 µg/mL, Invitrogen), β-mercaptoethanol (50 µM, Sigma-Aldrich), L-glutamine (2mM, Invitrogen), human apo-transferrin (20 µg/mL, Sigma-Aldrich) depleted for IgG using protein A sepharose (GE Healthcare). The next day, naive B cells were sorted and 250 naive B cells/well were co-cultured with the seeded 3T3-CD40L expressing cells in the presence of IL-4 (25ng/ml; Peprotech) and IL-21 (50ng/ml; Peprotech) for 3 – 11 days to determine proliferation, isotype switching, GC, memory and plasma cell formation and Ig production. Cultures were maintained at 37°C in an atmosphere with 5% pCO_2 and 21%, 3% or 1% pO_2. For some cultures after 3, 5 or 7 days cultures were moved from 1 to 3% pO_2 and vice versa.

Flow cytometry

Extracellular staining of surface markers

Cultured cells were washed with PBA and extracellular staining was performed at 4°C for 30 minutes using the following antibody conjugates; CD19 (562947), CD38 (646851), IgD (561315), and IgM (562977), CD138 (552723), CD21 (561372 or 740395), FAS/CD95 (762346), CD80 (750440 or 558226), CD86 (748375 or 562433), CXCR4 (563924) from BD Biosciences. IgG (M1268) from Sanquin Reagents. IgA (2050-09) from SouthernBiotech. CD27 (25-0279-42) from ThermoFisher. PNA (FL-1071-5) from VectorLabs. Glut1 (FAB1418A) from R&D. LIVE/DEAD Fixable Near-IR from Invitrogen.

Intracellular staining of signaling and transcription factors

Staining procedures were performed as previously described (59). In short, harvested and pooled cultures were kept on melting ice at all times. After washing, cultures were stained for membrane markers in a 25µl staining mix containing the Live/Dead stain, anti-CD19 and anti-CD38 antibodies. TF stain procedure also contained anti-CD27 antibodies during membrane marker staining. After staining, samples were washed once with ice-cold PBA and centrifuged. Samples were fixed with either paraformaldehyde (PFA; Sigma) or Foxp3 fixation buffer (eBioscience). PFA fixed samples were subsequently washed once and permeabilized with 90% methanol. Samples were incubated at -20°C till day of FACS analysis. Foxp3-fixed samples were washed once with Foxp3 permeabilization buffer and kept in ice-cold PBA in the dark till day of FACS analysis.

Before FACS analysis, all samples were retrieved from -20 °C or 4 °C storage and washed once with ice-cold PBA. Methanol permeabilized samples were washed once more before adding

25µl staining mix containing antibodies against STAT3 (564133, BD), pSTAT3 (612569, BD), NFκB p65 (565446, BD), STAT6 (IC2167T, R&D), pSTAT6 (612600, BD) and C-MYC (13871S, CST), NFκB p65, HIF1α (359706, Biolegend) diluted in PBA. Samples were incubated for 45 minutes on a plate shaker at room temperature. Afterwards, samples were washed once with PBA and measured on a flow cytometer.

Foxp3 fixed samples were washed once with Foxp3 permeabilization buffer. Samples were stained in 25µl staining mix containing antibodies against PAX5 (649708, Biolegend), BCL6 (358512, Biolegend), IRF4 (646416, Biolegend) and AID (565785, BD) or PAX5, BCL6, IRF4, BLIMP1 (IC36081R-025, R&D) and XBP-1s (562820, BD) diluted in Foxp3 permeabilization buffer and incubated for 30 minutes in the fridge. Samples were washed once with Foxp3 permeabilization buffer and measured on a flow cytometer.

All antibodies used have been tested prior to experiments in target positive and negative cell lines/PMBCs/total CD19+ cells and were diluted to optimal staining concentrations. For overall population shifts the gMFI was plotted and expression frequencies were plotted when there was a particular expansion of high- or low-expressing cells. Samples were measured on the BD LSR Fortessa or BD FACSymphony and analyzed using Flowjo V10.8. For representative gating strategy, see Figure S1.

Proliferation assays

B cells were labelled with proliferation dye according to manufacturer's instructions. In short, sorted B cells were washed with 10 ml PBS twice and resuspended to a concentration of 2×10^7 cells/ml in PBS. Cells and 4µM Violet Proliferation Dye 450 (VPD450, BD Biosciences) in PBS were mixed at a 1:1 ratio and incubated 15 minutes in a 37°C water bath in the dark, vortexing the tube every 5 minutes to ensure uniform staining. Cells were washed twice using a 10 times volume of cold culture medium to end labeling. Thereafter, B cells were cultured according to the protocol described above.

Assessment of B cell metabolic status

To monitor B cell metabolic activity, cells were cultured as described and loaded with 50nM MitoTracker Red CMXRos (M7512, Invitrogen) and 25nM MitoTracker Green FM (M7514, Invitrogen), 20nM BODIPY^{TM} FL C12 (4,4-Difluoro-5,7-Dimethyl-4-Bora-3a,4a-Diaza-s-Indacene-3-Dodecanoic Acid) (D3822, Invitrogen) or 200µM 2-NBDG (2-(N-(7-Nitrobenz-2-oxa-1,3-diazol-4-yl)Amino)-2-Deoxyglucose) (N13195, Invitrogen) for 30 minutes or 2.5uM MitoSOX (M36008, Invitrogen) for 10 minutes at 37 °CC 5% CO_2 in pre-warmed Hank's Buffered Salt Solution (HBSS, 14025050, Gibco) on day 0 and 7 of culture. Cells were washed, stained for membrane markers as described above and measured on a flow cytometer. Within experiments, for each sample, cell size was determined

using FSC/SCC and gMFI was corrected subsequently according to the average cell size.

Cell counts

Before FACS analysis samples were mixed with at least 10.000 CountBright Absolute counting beads (Thermo Fisher Scientific) and prepared for flow cytometry analysis as described above. Absolute B cell counts were determined according to the formula:

$$\frac{\#LiveCD19+}{\#Beadsmeasured}x\#beadsadded$$

Ig ELISAs of culture supernatants

IgM, IgA, IgG, and IgG1 and IgG4 expression levels were measured in culture supernatants at day 7, 11 and 14. 96-well maxisorb plates were coated with monoclonal mouse anti-human IgM (2µg/ml, MH15-1), anti-IgA (1µg/ml, MH14-01), anti-IgG (2µg/ml, MH16-1), anti-IgG1 (1µg/ml, MH161-01), and IgG4 (1µg/ml, MH164-01) in PBS all provided by Sanquin Reagents. Culture supernatants were incubated for 1h and secreted Igs were detected using 1µg/ml HRP-conjugated mouse anti-human IgM, IgA, IgG, IgG1, or IgG4 (Sanquin Reagents) in HPE (Sanquin Reagents). The ELISA was developed using TMB substrate, stopped by addition of 2M H_2SO_4 and absorbance was measured at 450 and 540 nm. OD values were normalized to values of a titration curve of a serum pool that was included in each plate.

Lactate production

L(+)-lactate production was measured in B cell culture supernatant using L-lactate Assay Kit (ab65331, Abcam) according to manufacturer's instructions. Lactate production was corrected for cell counts as measured by flow cytometry.

Real-time semi-quantitative RT-PCR

RNA isolation was performed as described elsewhere (60). Primers were developed to span exon–intron junctions and then validated (IL-4R: 5'- CCCTGAAGTCTGGGATTTCCT -3'). Gene expression levels were measured in duplicate reactions for each sample in StepOnePlus (Applied Biosystems, Foster City, CA, USA) using the SYBR green method (Applied Biosystems, Foster City, CA, USA). Expression of housekeeping gene 16S was used for normalization.

Statistical analysis

Statistical analysis was performed using GraphPad Prism 8. Data were analyzed using Repeated Measures one-way ANOVA with Tukey's multiple comparison test, Repeated Measures two-way ANOVA with Sidak's multiple comparison test or mixed-effects analysis with Dunnett's multiple comparison test where appropriate. Results were considered significant at p <0.05. Significance was depicted as *p <0.05 or **p <0.01, ***p <0.001 or ****p <0.0001. To show significance between specific datasets within a graph containing multiple datasets, the * shows the significance between the dataset matching the color of * and the dataset closest to the *.

Data availability statement

The original contributions presented in the study are included in the article/Supplementary material. Further inquiries can be directed to the corresponding author.

Ethics statement

The studies involving human participants were reviewed and approved by Sanquin Medical Ethical Committee. The patients/participants provided their written informed consent to participate in this study.

Author contributions

JK, CM, JS, ST, AB, SH, and TR designed research. JK, CM, JS, ST, and ND performed research. JK, CM and JS analyzed data. JK, CM, JS, AB, SH, and TR wrote the paper. All authors critically reviewed the manuscript, gave final approval of the version to be published, and agreed to be accountable for all aspects of the work ensuring that questions related to the accuracy or integrity of any part of the work are appropriately investigated and resolved.

Conflict of interest

The authors declare that the research was conducted in the absence of any commercial or financial relationships that could be construed as a potential conflict of interest.

Publisher's note

All claims expressed in this article are solely those of the authors and do not necessarily represent those of their affiliated organizations, or those of the publisher, the editors and the reviewers. Any product that may be evaluated in this article, or claim that may be made by its manufacturer, is not guaranteed or endorsed by the publisher.

Supplementary material

The Supplementary Material for this article can be found online at: https://www.frontiersin.org/articles/10.3389/fimmu.2022.1082154/full#supplementary-material

References

1. Elsner RA, Shlomchik MJ. Germinal center and extrafollicular b cell responses in vaccination, immunity and autoimmunity. *Immunity* (2020) 53 (6):1136–50. : doi: 10.1016/j.immuni.2020.11.006

2. Weisel FJ, Zuccarino-Catania GV, Chikina M, Shlomchik MJ. A temporal switch in the germinal center determines differential output of memory b and plasma cells. *Immunity* (2016) 44(1):116–30. doi: 10.1016/j.immuni.2015.12.004

3. Laidlaw BJ, Cyster JG. Transcriptional regulation of memory b cell differentiation. *Nat Rev Immunol* (2021) 21(4):209–20. doi: 10.1038/s41577-020-00446-2

4. Suan D, Kräutler NJ, Maag JLV, Butt D, Bourne K, Hermes JR, et al. CCR6 defines memory b cell precursors in mouse and human germinal centers, revealing light-zone location and predominant low antigen affinity. *Immunity* (2017) 47 (6):1142–1153.e4. doi: 10.1016/j.immuni.2017.11.022

5. Cunningham AF, Gaspal F, Serre K, Mohr E, Henderson IR, Scott-Tucker A, et al. Salmonella induces a switched antibody response without germinal centers that impedes the extracellular spread of infection. *J Immunol* (2007) 178(10):6200–7. doi: 10.4049/jimmunol.178.10.6200

6. Marshall JL, Zhang Y, Pallan L, Hsu M-C, Khan M, Cunningham AF, et al. Early b blasts acquire a capacity for ig class switch recombination that is lost as they become plasmablasts. *Eur J Immunol* (2011) 41(12):3506–12. doi: 10.1002/eji.201141762

7. Roco JA, Mesin L, Binder SC, Nefzger C, Gonzalez-Figueroa P, Canete PF, et al. Class switch recombination occurs infrequently in germinal centers. *Immunity* (2019) 51(2):337–50. doi: 10.1016/j.immuni.2019.07.001

8. Victora GD, Nussenzweig MC. Germinal centers. *Immunol Rev* (2022) 247 (1):5–10. doi: 10.1146/annurev-immunol-120419-022408

9. Shinnakasu R, Inoue T, Kometani K, Moriyama S, Adachi Y, Nakayama M, et al. Regulated selection of germinal-center cells into the memory b cell compartment. *Nat Immunol* (2016) 17(7):861–9. doi: 10.1038/ni.3460

10. Laidlaw BJ, Schmidt TH, Green JA, Allen CDC, Okada T, Cyster JG. The eph-related tyrosine kinase ligand ephrin-B1 marks germinal center and memory precursor b cells. *J Exp Med* (2017) 214(3):639–49. doi: 10.1084/jem.20161461

11. Takahashi Y, Dutta PR, Cerasoli DM, Kelsoe G. *In situ* studies of the primary immune response to (4-Hydroxy-3-Nitrophenyl)Acetyl. v. affinity

maturation develops in two stages of clonal selection.. *J Exp Med* (1998) 187 (6):885–95. doi: 10.1084/jem.187.6.885

12. Unger PPA, Verstegen NJM, Marsman C, Jorritsma T, Rispens T, Ten Brinke A, et al. Minimalistic *In vitro* culture to drive human naive b cell differentiation into antibody-secreting cells. *Cells* (2021) 10(5):1183. doi: 10.3390/cells10051183

13. Linterman MA, Beaton L, Yu D, Ramiscal RR, Srivastava M, Hogan JJ, et al. IL-21 acts directly on b cells to regulate bcl-6 expression and germinal center responses. *J Exp Med* (2010) 207(2):353–63. doi: 10.1084/jem.20091738

14. Tangye SG, Ferguson A, Avery DT, Ma CS, Hodgkin PD. Isotype switching by human b cells is division-associated and regulated by cytokines. *J Immunol* (2002) 169(8):4298–306. doi: 10.4049/jimmunol.169.8.4298

15. Zotos D, Coquet JM, Zhang Y, Light A, D'Costa K, Kallies A, et al. IL-21 regulates germinal center b cell differentiation and proliferation through a b cell-intrinsic mechanism. *J Exp Med* (2010) 207(2):365–78. doi: 10.1084/jem.20091777

16. Tellier J, Nutt SL. Plasma cells: The programming of an antibody-secreting machine.*Eur J Immunol* (2019) 49(1):30–7.

17. Nutt SL, Hodgkin PD, Tarlinton DM, Corcoran LM. The generation of antibody-secreting plasma cells. *Nat Rev Immunol* (2015) 15(3):160–71. doi: 10.1038/nri3795

18. Klein U, Casola S, Cattoretti G, Shen Q, Lia M, Mo T, et al. Transcription factor IRF4 controls plasma cell differentiation and class-switch recombination. *Nat Immunol* (2006) 7(7):773–82. doi: 10.1038/ni1357

19. Ding BB, Bi E, Chen H, Yu JJ, Ye BH. IL-21 and CD40L synergistically promote plasma cell differentiation through upregulation of blimp-1 in human b cells. *J Immunol* (2013) 190(4):1827–36. doi: 10.4049/jimmunol.1201678

20. Avery DT, Deenick EK, Ma CS, Suryani S, Simpson N, Chew GY, et al. B cell-intrinsic signaling through IL-21 receptor and STAT3 is required for establishing long-lived antibody responses in humans. *J Exp Med* (2010) 207 (1):155–71. doi: 10.1084/jem.20091706

21. Craxton A, Shu G, Graves JD, Saklatvala J, Krebs EG, Clark EA. p38 MAPK is required for CD40-induced gene expression and proliferation in b lymphocytes. *J Immunol* (1998) 161(7):3225–36.

22. Sun SC. The non-canonical NF-κB pathway in immunity and inflammation. *Vol. 17 Nat Rev Immunol Nat Publishing Group;* (2017), 545–58. doi: 10.1038/nri.2017.52

23. Chen D, Ireland SJ, Remington G, Alvarez E, Racke MK, Greenberg B, et al. CD40-mediated NF-κB activation in b cells is increased in multiple sclerosis and modulated by therapeutics. *J Immunol* (2016) 197(11):4257–65. doi: 10.4049/jimmunol.1600782

24. Finkin S, Hartweger H, Oliveira TY, Kara EE, Nussenzweig MC. Protein amounts of the MYC transcription factor determine germinal center b cell division capacity. *Immunity* (2019) 51(2):324–336.e5. doi: 10.1016/j.immuni.2019.06.013

25. Luo W, Weisel F, Shlomchik MJ. B cell receptor and CD40 signaling are rewired for synergistic induction of the c-myc transcription factor in germinal center b cells. *Immunity* (2018) 48(2):313–326.e5. doi: 10.1016/j.immuni.2018.01.008

26. Calado DP, Sasaki Y, Godinho SA, Pellerin A, Köchert K, Sleckman BP, et al. The cell-cycle regulator c-myc is essential for the formation and maintenance of germinal centers. *Nat Immunol* (2012) 13(11):1092–100. doi: 10.1038/ni.2418

27. Dominguez-Sola D, Victora GD, Ying CY, Phan RT, Saito M, Nussenzweig MC, et al. The proto-oncogene MYC is required for selection in the germinal center and cyclic reentry. *Nat Immunol* (2012) 13(11):1083–91. doi: 10.1038/ni.2428

28. Kitano M, Moriyama S, Ando Y, Hikida M, Mori Y, Kurosaki T, et al. Bcl6 protein expression shapes pre-germinal center b cell dynamics and follicular helper T cell heterogeneity. *Immunity* (2011) 34(6):961–72. doi: 10.1016/j.immuni.2011.03.025

29. Harris MB, Chang C-C, Berton MT, Danial NN, Zhang J, Kuehner D, et al. Transcriptional repression of Stat6-dependent interleukin-4-Induced genes by BCL-6: Specific regulation of iε transcription and immunoglobulin e switching. *Mol Cell Biol* (1999) 19(10):7264–75. doi: 10.1128/MCB.19.10.7264

30. Atkuri KR, Herzenberg LA, Herzenberg LA. Culturing at atmospheric oxygen levels impacts lymphocyte function. *Proc Natl Acad Sci U S A.* (2005) 102(11):3756–9. doi: 10.1073/pnas.0409910102

31. Burrows N, Maxwell PH. Hypoxia and b cells. *Exp Cell Res* (2017) 356 (2):197–203. doi: 10.1016/j.yexcr.2017.03.019

32. Cho SH, Raybuck AL, Stengel K, Wei M, Beck TC, Volanakis E, et al. Germinal centre hypoxia and regulation of antibody qualities by a hypoxia response system. *Nature* (2016) 537(7619):234–8. doi: 10.1038/nature19334

33. Cho SH, Raybuck AL, Blagih J, Kemboi E, Haase VH, Jones RG, et al. Hypoxia-inducible factors in CD4+ T cells promote metabolism, switch cytokine secretion, and T cell help in humoral immunity. *Proc Natl Acad Sci U S A.* (2019) 116(18):8975–84. doi: 10.1073/pnas.1811702116

34. Abbott RK, Thayer M, Labuda J, Silva M, Philbrook P, Cain DW, et al. Germinal center hypoxia potentiates immunoglobulin class switch recombination. *J Immunol* (2016) 197(10):4014–20. doi: 10.4049/jimmunol.1601401

35. Burrows N, Bashford-Rogers RJM, Bhute VJ, Peñalver A, Ferdinand JR, Stewart BJ, et al. Dynamic regulation of hypoxia-inducible factor-1α activity is essential for normal b cell development. *Vol. 21 Nat Immunol* (2020) p:1408–20. doi: 10.1038/s41590-020-0772-8

36. Jellusova J, Cato MH, Apgar JR, Ramezani-Rad P, Leung CR, Chen C, et al. Gsk3 is a metabolic checkpoint regulator in b cells. *Nat Immunol* (2017) 18(3):303–12. doi: 10.1038/ni.3664

37. Halligan DN, Murphy SJE, Taylor CT. The hypoxia-inducible factor (HIF) couples immunity with metabolism. *Semin Immunol [Internet]*. (2016) 28(5):469–77. doi: 10.1016/j.smim.2016.09.004

38. Li L, Feng C, Qin J, Li D, Liu M, Han S, et al. Regulation of humoral immune response by HIF-1α-dependent metabolic reprogramming of the germinal center reaction. *Cell Immunol* (2021), 367. doi: 10.1016/j.cellimm.2021.104409

39. Firmino NS, Cederberg RA, Lee C-M, Shi R, Wadsworth BJ, Franks SE, et al. Germinal center hypoxia in tumor-draining lymph nodes negatively regulates tumor-induced humoral immune responses in mouse models of breast cancer. *Oncoimmunology* (2021) 10(1):1959978. doi: 10.1080/2162402X.2021.1959978

40. Weisel FJ, Mullett SJ, Elsner RA, Menk AV, Trivedi N, Luo W, et al. Germinal center b cells selectively oxidize fatty acids for energy while conducting minimal glycolysis. *Nat Immunol* (2020) 21(3):331–42. doi: 10.1038/s41590-020-0598-4

41. Koers J, Pollastro S, Tol S, Pico-knijnenburg I, Derksen NIL, Van SPA, et al. CD45RB glycosylation and ig isotype define maturation of functionally distinct b cell subsets in human peripheral blood. *Front Immunol* (2022) 13(April):1–8. doi: 10.3389/fimmu.2022.891316

42. Marsman C, Verhoeven D, Koers J, Rispens T. Optimized protocols for *in vitro* T cell-dependent and T cell- independent activation for b cell differentiation studies using limited cells. *Front Immunol* (2022) 29(13):815449. doi: 10.3389/fimmu.2022.815449

43. Pearce EL, Pearce EJ. Metabolic pathways in immune cell activation and quiescence. *Immunity* (2013) 38(4):633–43. doi: 10.1016/j.immuni.2013.04.005

44. Verstegen NJM, Ubels V, Westerhoff HV, van Ham SM, Barberis M. System-level scenarios for the elucidation of T cell-mediated germinal center b cell differentiation. *Front Immunol* (2021) 12(September):1–19. doi: 10.3389/fimmu.2021.734282

45. Victora GD, Schwickert TA, Fooksman DR, Kamphorst AO, Meyer-Hermann M, Dustin ML, et al. Germinal center dynamics revealed by multiphoton microscopy with a photoactivatable fluorescent reporter. *Cell* (2010) 143(4):592–605. doi: 10.1016/j.cell.2010.10.032

46. Allen CDC, Ansel KM, Low C, Lesley R, Tamamura H, Fujii N, et al. Germinal center dark and light zone organization is mediated by CXCR4 and CXCR5. *Nat Immunol* (2004) 5(9):943–52. doi: 10.1038/ni1100

47. Heise N, De Silva NS, Silva K, Carette A, Simonetti G, Pasparakis M, et al. Germinal center b cell maintenance and differentiation are controlled by distinct NF-κB transcription factor subunits. *J Exp Med* (2014) 211(10):2103–18. doi: 10.1084/jem.20132613

48. Cobaleda C, Schebesta A, Delogu A, Busslinger M. Pax5: The guardian of b cell identity and function. *Vol. 8 Nat Immunol* (2007), 463–70. doi: 10.1038/ni1454

49. Vander Heiden MG, Cantley LC, Thompson CB. Understanding the warburg effect: the metabolic requirements of cell proliferation. *Science* (2009) 324(5930):1029–33. doi: 10.1126/science.1160809

50. Halligan DN, Murphy SJE, Taylor CT. The hypoxia-inducible factor (HIF) couples immunity with metabolism. *Semin Immunol* (2016) 28(5):469–77.

51. Deenick EK, Avery DT, Chan A, Berglund LJ, Ives ML, Moens L, et al. Naive and memory human b cells have distinct requirements for STAT3 activation to differentiate into antibody-secreting plasma cells. *J Exp Med* (2013) 210(12):2739–53. doi: 10.1084/jem.20130323

52. Abe H, Semba H, Takeda N. The roles of hypoxia signaling in the pathogenesis of cardiovascular diseases. *J Atheroscler Thromb* (2017) 24(9):884–94. doi: 10.5551/jat.RV17009

53. Trayhurn P, Wang B, Wood IS. Hypoxia in adipose tissue: A basis for the dysregulation of tissue function in obesity? *Br J Nutr* (2008) 100(2):227–35. doi: 10.1017/S0007114508971282

54. Sun K, Zhang Y, D'Alessandro A, Nemkov T, Song A, Wu H, et al. Sphingosine-1-phosphate promotes erythrocyte glycolysis and oxygen release for adaptation to high-altitude hypoxia. *Nat Commun* (2016) 7:12086. doi: 10.1038/ncomms12086

55. Zamudio S, Borges M, Echalar L, Kovalenko O, Vargas E, Torricos T, et al. Maternal and fetoplacental hypoxia do not alter circulating angiogenic growth effectors during human pregnancy. *Biol Reprod* (2014) 90(2):42. doi: 10.1095/biolreprod.113.115592

56. Carreau A, El Hafny-Rahbi B, Matejuk A, Grillon C, Kieda C. Why is the partial oxygen pressure of human tissues a crucial parameter? small molecules and hypoxia. *J Cell Mol Med* (2011) 15(6):1239–53. doi: 10.1111/j.1582-4934.2011.01258.x

57. Schito L, Semenza GL. Hypoxia-inducible factors: Master regulators of cancer progression. *Trends cancer.* (2016) 2(12):758–70. doi: 10.1016/j.trecan.2016.10.016

58. Brown JM. Exploiting tumour hypoxia and overcoming mutant p53 with tirapazamine. *Br J Cancer.* (1998) 77 Suppl 4(Suppl 4):12–4. doi: 10.1038/bjc.1998.430

59. Marsman C, Jorritsma T, Ten Brinke A, van Ham SM. Flow cytometric methods for the detection of intracellular signaling proteins and transcription factors reveal heterogeneity in differentiating human b cell subsets. *Cells* (2020) 9:2633. doi: 10.3390/cells9122633

60. Souwer Y, Chamuleau MED, Van De Loosdrecht AA, Tolosa E, Jorritsma T, Muris JJF, et al. Detection of aberrant transcription of major histocompatibility complex class II antigen presentation genes in chronic lymphocytic leukaemia identifies HLA-DOA mRNA as a prognostic factor for survival. *Br J Haematol [Internet].* (2009) 145(3):334–43. doi: 10.1111/j.1365-2141.2009.07625.x